ORIGINAL ARTICLE

A setting-round process of pipe end by three-roller for large pipes

Qingdang Meng[1,2] · Shiqi Zhang[1,2] · Ruixue Zhai[1,2] · Pengcheng Fu[1,2] · Jun Zhao[1,2]

© The Author(s), under exclusive licence to Springer-Verlag London Ltd., part of Springer Nature 2022

Abstract
Ovality is one of the important quality parameters of pipes. If ovality does not meet the standard, the performance and life of pipes will be affected. In order to improve the quality of pipe connections, ovality of pipe ends has higher requirements. Since existing processes cannot achieve continuous and high-efficiency setting-round of pipe ends, this study proposed a three-roller setting-round process for pipe ends. Experiments and numerical simulations were performed to verify the feasibility of the process. In simulations, the Bauschinger effect, the variation of chord modulus, and the yield plateau phenomenon were considered. The results show that residual ovality of the straight pipes, elbow, and tee pipe after setting-round is less than 1%, which is in line with the API standard. Residual ovality of pipe ends decreases with the increase of the reduction, and tends to be stable after reaching the optimum reduction. There is an approximate linear relationship between the relative thickness and the optimal reduction. With the increase of the relative thickness, the optimal reduction shows a downward trend. The proposed process can realize continuous setting-round of pipe ends of straight pipes, elbows, and tee pipes, and improve the setting-round efficiency. In addition, the setting of process parameters is independent of initial ovality, and the process is simple to realize.

1 Introduction

In recent years, pipeline transportation with large capacity, low energy consumption, and airtight safety has become the most important transportation mode of oil and natural gas. According to different shapes and functions, oil and gas transportation pipes can be divided into straight pipes, tees, elbows, and other types. Various pipes must be connected in a certain way to form a complete pipeline transportation system. Therefore, in order to meet the docking and assembly requirements of pipes in severe working conditions, ovality of pipe ends must be strictly regulated. The API Spec 5L standard [1] proposed by American Petroleum Institute stipulates that ovality of the pipe body of steel pipe products for pipelines cannot exceed 1.5% of the nominal diameter, and ovality of the pipe ends cannot exceed 1.0% of the nominal diameter. In actual production, it often occurs that ovality of the pipe body meets the standard, but only ovality of the pipe ends does not meet the standard. At this time, the use of overall setting-round methods is low in efficiency and high in cost. Therefore, the development of an accurate and efficient pipe end setting-round process has become an urgent need for pipe manufacturers.

At present, setting-round processes of pipe ends mainly adopt methods of changing the diameter and over-bending. The method of changing diameter includes expanding and compression; that is, the diameter of pipes is expanded or compressed by applying force from the inside or outside of pipes. Karrech et al. [2] established a mathematical model

✉ Ruixue Zhai
  zhairuixue@ysu.edu.cn

  Qingdang Meng
  mengqingdangysu@163.com

  Shiqi Zhang
  zhangshiqi@stumail.ysu.edu.cn

  Pengcheng Fu
  pengchengfu@stumail.ysu.edu.cn

  Jun Zhao
  zhaojun@ysu.edu.cn

1 Key Laboratory of Advanced Forging & Stamping Technology and Science (Yanshan University), Ministry of Education of China, Qinhuangdao City, People's Republic of China

2 College of Mechanical Engineering, Yanshan University, No. 438, Hebei Street, Haigang District, P. O. Box 066004, Qinhuangdao City, People's Republic of China

for predicting the stress field distribution in the expanding zone, and provided a theoretical basis for the study of diameter expanding. Zhao et al. [3, 4] derived the springback theory of small curvature plane bending, and applied the theory to diameter expanding of pipes. Ji et al. [5] conducted a simulation study on the mechanical expanding process, and effect laws of the process parameters on the pipe quality were examined. However, the mechanical expanding machine has a complex structure and high cost. Therefore, Yin et al. [6] proposed the use of compression instead of expansion to achieve setting-round of pipes. After setting-round, ovality of the pipe ends is less than 0.12%. The equipment is simple in structure and low in cost. The expansion and compression process will change the circumference of pipes, so it is not suitable for the pipes whose size meets the standard and ovality does not meet the standard. In response to this problem, researchers have proposed the over-bending setting-round process [7, 8]. However, the operation of the over-bending method is complicated, and initial ovality needs to be detected first.

In addition, the roller setting-round process was developed for pipes with qualified circumference dimensions but unqualified ovality. Yu et al. [9] proposed the reciprocating bending uniform curvature theorem through theoretical analysis. The theory holds that the curvatures will be unified to the same value after micro-segments with different initial curvatures undergoing multiple reciprocating bending. This theorem is an important theoretical basis for the roller setting-round process. On the basis of the above theorem, the roller setting-round process for the whole pipe [10–13] has been proposed successively. The current roller setting-round process for the whole pipe has high efficiency and precision, but it cannot realize pipe end setting-round of special-shaped pipes such as elbows and tees.

The material model is one of the important factors affecting the accuracy of numerical simulation. In the roller setting-round processes, circumferential micro-segments of pipes undergo multiple cyclic bending, and the Bauschinger effect of the material needs to be considered. Prager [14] and Ziegler [15] first proposed the linear kinematic hardening model. Mroz [16] proposed a multi-yield surface model, which uses piecewise linearity to fit the response curve. Armstrong and Frederick [17] added a dynamic recovery term in the evolution of back stress, which can better describe the nonlinear plastic behavior of materials. Chaboche [18] decomposed the back stress into multiple, and each back stress component still follows the A-F hardening model. Combined with the isotropic hardening model, the Chaboche model has a high description accuracy for the hysteresis curve and has been widely used. According to characteristics of X70, X80, and X90 pipeline steel materials, Zou et al. [19] established a Chaboche combined hardening model that comprehensively considered the Bauschinger effect, the variation of chord modulus, and the yield plateau phenomenon, and used it for UOE steel pipe forming process. Zobec et al. [20] used the Chaboche combined hardening model to reasonably predict the residual stress relaxation under cyclic loading. Hai et al. [21] proposed a method to quickly calibrate material parameters of the Chaboche hardening model for the low yield point steel, low carbon steel, and high strength steel. In addition, a large number of scholars have found that the unloading–reloading response of the material after plastic deformation is no longer a straight line, but a slight curve. Yoshida et al. [22] used chord modulus to approximate nonlinear unloading–reloading curves and proposed an empirical expression for chord modulus as a function of plastic strain. The chord modulus model has been widely used [23–25], and the research results have shown that the use of the chord modulus model can significantly improve the springback prediction accuracy.

In summary, none of the existing setting-round processes can achieve efficient and accurate pipe end setting-round for elbows, tee pipes, and straight pipes. In addition, most of existing setting-round process researches use over-simplified material models, which restrict the improvement of simulation accuracy. In view of the above problems, this study proposed a setting-round process of pipe ends by three-roller. Numerical simulations and experiments were carried out to verify the feasibility of the process. The Bauschinger effect, the variation of chord modulus and the yield plateau phenomenon of materials were considered. Effects of different factors on the setting-round results were explored. The new setting-round process makes up for the shortcomings of the existing setting-round processes and can achieve accurate and efficient pipe end setting-round for different types of pipe fittings. The process is simple to implement and can be used for on-site real-time setting-round. In addition, the material model used in numerical simulations can provide reference for other processes involving reciprocating loading.

2 Process introduction

2.1 Setting-round procedure

The process can be divided into the initial stage, the setting-round stage, and the unloading stage according to time sequence, as shown in Fig. 1.

Figure 1a shows the initial stage. The three rollers have a certain taper and are mounted on the turntable. The distances between the three rollers and the center of the turntable are the same, and the angle formed by any two rollers and the center of the turntable is 120°. The pipe is fixed and can only
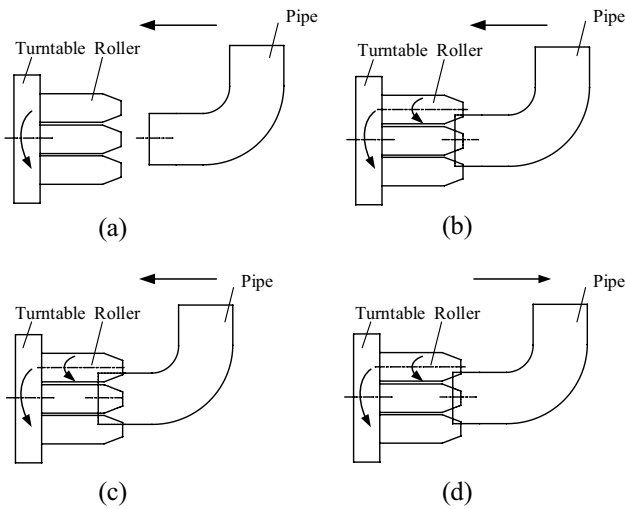
Fig. 1 Process flow: **a** the initial stage, **b**, **c** the setting-round stage, **d** the unloading stage

be displaced in the direction of the turntable. In the initial stage, the pipe begins to move toward the turntable, and the turntable rotates so that the rollers can rotate around the pipe end. Figure 1b and c show the setting-round stage. During the advancing process of the pipe, the pipe end is in contact with the taper and the straight part of the roller in turn. When it is in contact with the straight part, the reduction reaches the maximum. After advancing a certain distance, the pipe moves in the opposite direction, and the pipe is still in contact with the straight part of the roller. Figure 1d shows the unloading stage. During the reverse movement of the pipe to the initial position, the reduction gradually decreases, and the radial force gradually decreases until the pipe is separated from the rollers.

This process is based on the reciprocating bending uniform curvature theorem [21], that is, multiple reciprocating bending can eliminate the difference in initial curvature, and finally make the curvature unified to the same direction and the same value. Here, it is stipulated that the bending curvature becomes larger as positive bending (PB), and the bending curvature becomes smaller as reverse bending (RB). In order to illustrate the reciprocating bending process experienced by the pipe fitting, the cross-section of the pipe fitting is selected for research. Figure 2 shows the deformation path of points in a pipe along the circumferential direction.

The deformation state of a pipe at a certain time during the setting-round process is shown in Fig. 2a. The pipe produces three positive bending areas and three reverse bending areas under the action of the three rollers. The subsequent deformation is discussed taking point A as an example. Point A switches from reverse bending to positive bending when the roller 1 moves from point A to point B, as shown in Fig. 2b. Three rollers rotate once, and the path of roller 1 is A-B-C-D-E–F-A, then point A has experienced RB-PB-RB-PB-RB-PB-RB. Similarly, the deformation process of any point can be analyzed. When the three rollers revolve around the pipe, any point on the pipe undergoes three reciprocating bending. In the setting-round stage, the circumferential micro-segments of the pipe end undergo PB and RB alternately, and the curvatures of the positive and reverse bending areas are unified into two values. During the continuous unloading process, the positive bending curvature gradually decreases, and the reverse bending curvature gradually increases. When the unloading reaches a certain moment, the curvature of the two areas after springback is just the nominal curvature, and pipes are rounded.

Fig. 2 Schematic diagram of the deformation of circumferential micro-segments: (**a**) before the position change of the three rollers, (**b**) after the position change of the three rollers
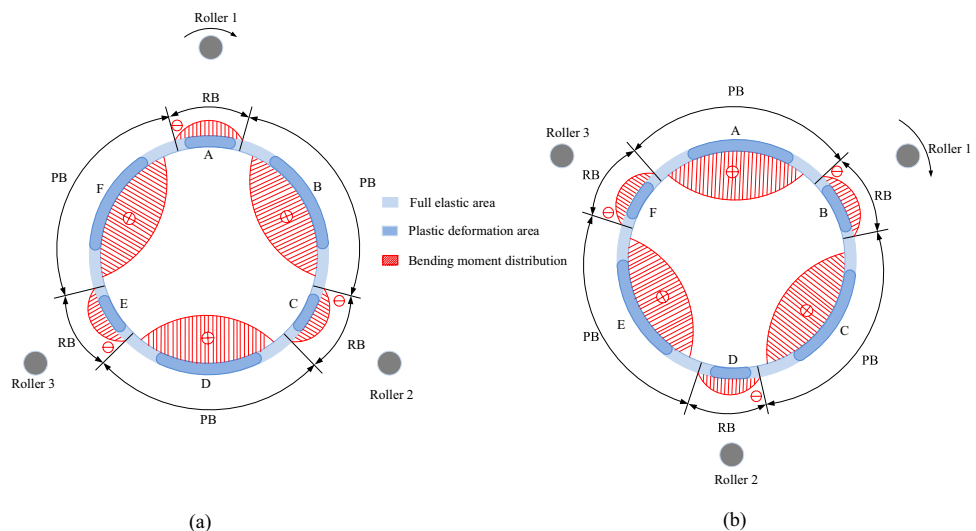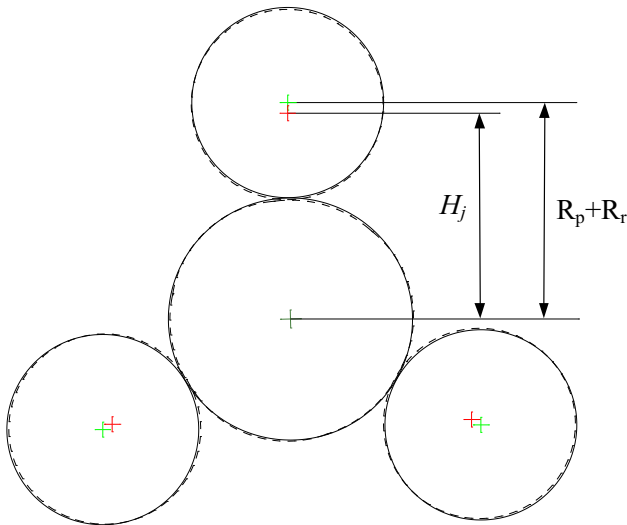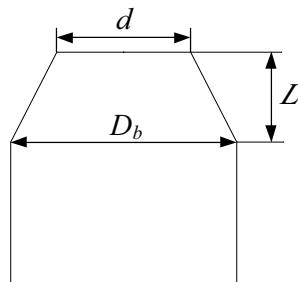
Fig. 3 Schematic diagram of the reduction

Fig. 4 Schematic diagram of roll size

2.2 Process parameters

The process involves the following process parameters.

(1) Reduction

As shown in Fig. 3, the reduction is the radial distance of each roller toward the center of the pipe. The reduction of the three rollers is the same, and the reduction is recorded as H. The calculation expression is as follows

$$H = R_p + R_r - H_j \tag{1}$$

where H is the reduction (mm); R_p is the radius of the pipe end (mm); R_r is the radius of the roller (mm); H_j is the radial distance between the center of the roller and the center of the pipe (mm).

(2) Roller taper

As shown in Fig. 4, the calculation expression of the roller taper is given by

$$C = \frac{D_b - d}{L} \tag{2}$$

where C is the taper of the roller; D_b is the maximum diameter of the roller (mm); d is the minimum diameter of the roller (mm); L is the height of the frustum of a cone (mm).

(3) Revolution speed and forward speed

The revolution speed refers to the rotational speed of the turntable (r/s). The forward speed refers to the displacement speed of the pipe in the direction of the turntable (mm/s). Unless otherwise specified, the revolution speed is 0.2 r/s.

(4) Setting-round length

The setting-round length is the maximum length of the straight section of the roller in contact with the pipe. The setting-round length is determined according to the API standard and actual production needs. Unless otherwise specified, the following setting-round lengths are all 10 mm.

(5) Ovality

The ovality is used to measure the quality of the setting-round. The ovality is defined as

$$\delta = \frac{2(a - b)}{D} \times 100\% \tag{3}$$

where a is the radius of the major axis of the ellipse (mm); b is the radius of the minor axis of the ellipse (mm); D is the nominal outer diameter of the pipe (mm).

(6) Relative thickness

The relative thickness M is defined as the ratio of the wall thickness of the pipe to the nominal outer diameter, and its calculation expression is given by

$$M = \frac{t}{D} \tag{4}$$

where M is the relative thickness; t is the wall thickness of the pipe fitting (mm); D is the nominal outer diameter of the pipe fitting (mm).

3 Constitutive model

Based on the von Mises yield criterion and the Chaboche combined hardening model, the yield function can be expressed as

$$F = \tilde{\sigma} - Y = 0 \tag{5}$$

where $\tilde{\sigma}$ is the equivalent stress and Y is the yield stress.

Under the von Mises yield criterion, the equivalent stress expression is

$$\tilde{\sigma} = \sqrt{\frac{3}{2}(s - \alpha) : (s - \alpha)} \qquad (6)$$

where s is the deviatoric stress tensor and α is the back stress tensor.

In the Chaboche model [18], the back stress can be decomposed into multiple, and the number of back stresses is taken as 3.

$$\alpha = \sum_{i=1}^{3} \alpha_i \qquad (7)$$

Each back stress follows the A-F evolution criterion [17]

$$d\alpha_i = \frac{2}{3} C_i d\varepsilon^p - \gamma_i \alpha_i dp \qquad (8)$$

where C_i and γ_i are the kinematic hardening parameters.

In order to describe the yield plateau phenomenon, Zou [19] proposed a new yield surface radius evolution model. The above model considers that the evolution criterion of the yield surface radius inside the yield plateau is different from that outside the yield plateau, and its expression is

$$\eta(p) = \begin{cases} \sigma_0 + (\sigma_a - \sigma_0) \cdot (1 - \exp(-b_0 p)), & p \leq \varepsilon_{pla} \\ \Psi + Q \cdot (1 - \exp(-bp)), & p \geq \varepsilon_{pla} \end{cases} \qquad (9)$$

where η is the size of the yield surface under a certain plastic strain p; σ_0 is the initial yield stress; σ_a, b_0, and Ψ are the material parameters describing the yield plateau; Q is the saturated stress of the isotropic hardening stress at infinite plastic strain; b determines the rate of isotropic hardening stress saturation; ε_{pla} is the yield plateau length.

Most metals exhibit significant nonlinearity in their unloading and reloading responses after undergoing plastic deformation, as shown in the Fig. 5. At this time, using the traditional constant elastic modulus, the error will be large. The accuracy can be significantly improved by using the chord modulus. Since the material in the proposed process undergoes multiple unloading and loading, the chord modulus model can improve the simulation accuracy of the process.

The calculation formula of the chord modulus is given by

$$E_{chord} = \frac{\sigma_b - \sigma_a}{\varepsilon_b - \varepsilon_a} \qquad (10)$$

where E_{chord} is the chord modulus; σ_b and ε_b are the stress and strain values at the point b; σ_a and ε_a are the stress and strain values at the point a.

To account for the chord modulus variation, the empirical expression proposed by Yoshida et al. [22] was used.
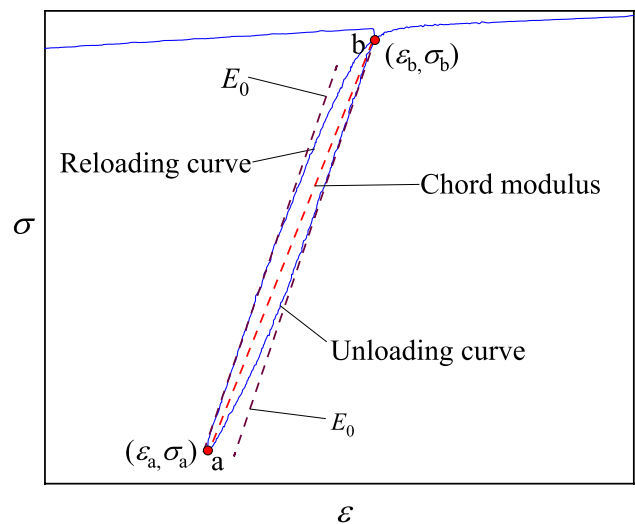

Fig. 5 Schematic diagram of nonlinear unloading–reloading

Table 1 X70 and X80 pipeline steel material parameters [19]

Material parameters	X70	X80
σ_0 (MPa)	530	600
σ_a (MPa)	377	380
Ψ (MPa)	203	325
E_0 (MPa)	233377	227000
E_a (MPa)	165122	163000
ε_{pla} (%)	4.1	2.0
C_1 (MPa)	928	22518
C_2 (MPa)	24181	97653
C_3 (MPa)	62148	836
γ_1	12	165
γ_2	225	1387
γ_3	2001	2
Q (MPa)	261	152
b	21	20
b_0	300	215
ξ_e	57	76

$$E_{chord} = E_0 - (E_0 - E_a)\left[1 - \exp(-\xi_e p)\right] \qquad (11)$$

where E_{chord} is the chord modulus under a certain plastic strain p; E_0 is the chord modulus under the initial condition; E_a represents the chord modulus under infinite pre-strain; ξ_e determines the speed at which the chord modulus decreases with the plastic strain.

The material parameters are referenced from literature [19]. The model parameters are shown in Table 1. The material response curve obtained from the hardening model is shown in Fig. 6.

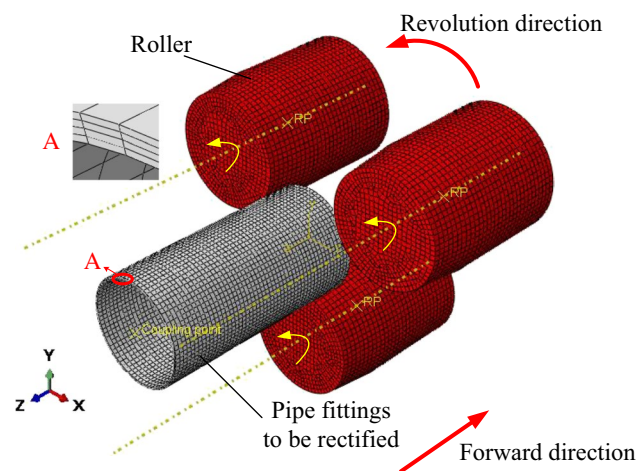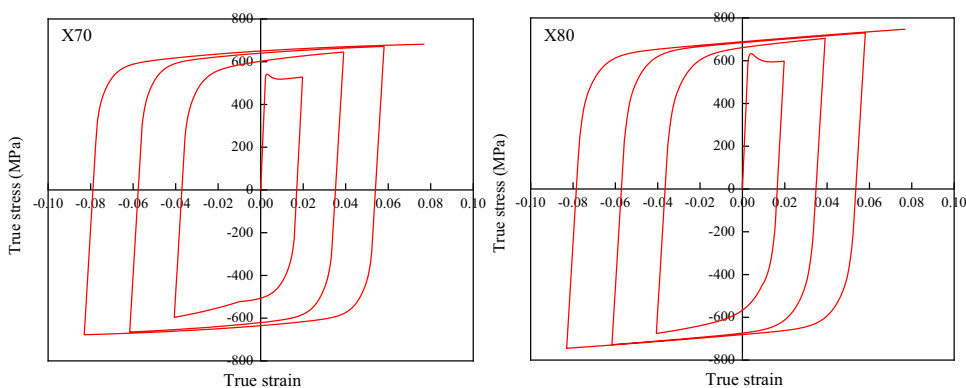**Fig. 6** Material response curve

Fig. 7 Finite element model

4 Finite element model

In the simulations, the size of the large pipes and the rollers is scaled according to the ratio of 10:1.

The setting-round process is simulated based on the dynamic implicit algorithm in the ABAQUS/Standard module, and the finite element model is shown in Fig. 7. The pipes are modeled as the deformable body, the mesh type is 8-node linear hexagonal incompatible module elements (C3D8I), the thickness direction is divided into 4 layers of mesh, and the other mesh size is 4 mm. The three rollers are discretized into rigid bodies with a mesh size of 5 mm. The contact between the pipe and the rollers is surface-to-surface contact, and the friction coefficient is 0.2. The center point of the end face of the pipe is coupled with the end face. The forward speed of the pipe is set to 2 mm/s. The revolution motion of the rollers is realized by the Periodic amplitude curve. The Periodic amplitude curve is represented by the Fourier series, and the Fourier series expression is given by

Table 2 Dimensions of straight pipe and rollers in pipe end setting-round process

D (mm)	t (mm)	L_p (mm)	D_b (mm)	C	L_r (mm)
140/120/100	2	200	120	0.2	200

where D is the nominal outer diameter of the pipe, t is the wall thickness, L_p is the pipe length, D_b is the diameter of the large end of the circular table, C is the taper of the roller, and L_r is the roller length

$$f(t) = \frac{a_0}{2} + \sum_{n=1}^{\infty} \left[a_n \, \cos \, n\omega_n t + b_n \, \sin \, n\omega_n t \right] \quad (12)$$

where $n = 1,2,3,\ldots$ positive integers; $\frac{a_0}{2}$ is the initial amplitude; ω_n is the circular frequency (rad/s); a_n is the coefficient of the cos term; b_n is the coefficient of the sin term.

The material parameters used in the finite element are shown in Table 1. The Chaboche hardening model is already built into ABAQUS. The improved isotropic hardening expression is a piecewise function, which is approximated by the connection of discrete points in ABAQUS. A point is taken every 0.01 plastic strain, and a total of 131 points are taken. In order to realize the variation of the chord modulus, it is necessary to write subroutines. The field variable subroutine "USDFLD" is written to read the plastic strain field and realize the variation of the chord modulus.

5 Finite element results and discussion

5.1 Straight pipe

5.1.1 Stress and strain analysis

The dimensions of the straight pipes and rollers used in the simulations are shown in Table 2.

The X70 material straight pipe with a length of 200 mm, a nominal outer diameter of 100 mm, a thickness of 2 mm, and an initial ovality of 3.14% at the pipe end was selected

Fig. 8 The equivalent stress distribution during the three-roller pipe end setting-round process

(a) Loading stage

(b) Setting-round stage

(c) Unloading stage

(d) After setting-round
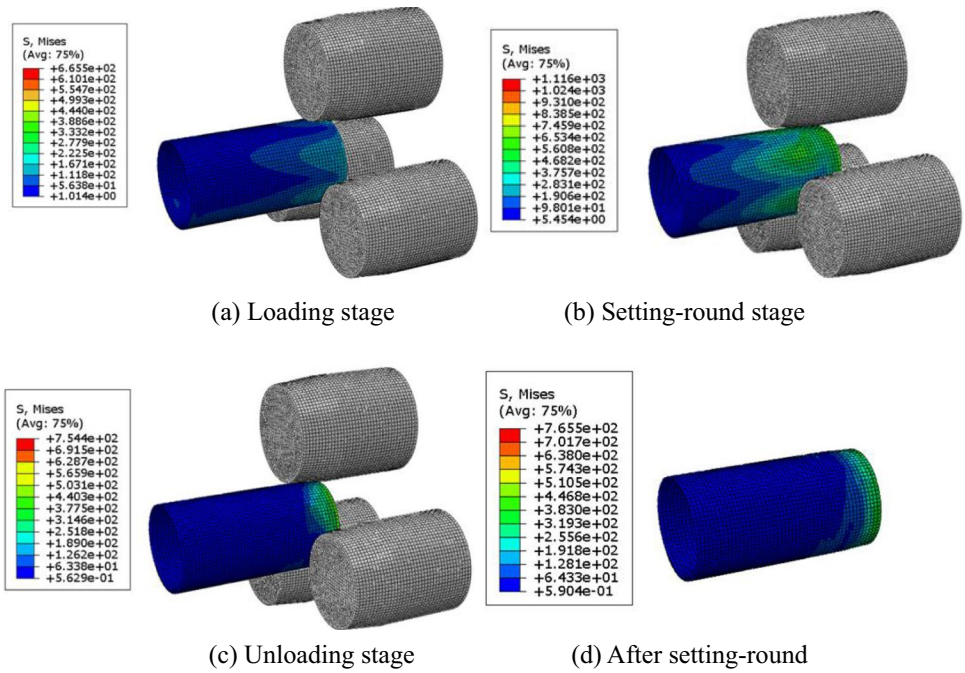
as the research object. Therefore, the three-roller pipe end setting-round process is analyzed in this case.

It can be seen from Fig. 8a that when the pipe end is in contact with the taper area of the rollers, the pipe end begins to be compressed radially. At this time, the pipe ends gradually transition from elastic deformation to elastoplastic deformation. It can be seen from Fig. 8b that when the pipe is in contact with the straight part of the rollers, the reduction reaches the maximum, and the plastic deformation is the largest. It can be seen from Fig. 8c that during unloading, the pipe end and the rollers are gradually separated, and the force gradually decreases. The equivalent stress distribution of the pipe after setting-round is shown in Fig. 8d. It can be seen from Fig. 8d that the pipe end and the pipe body are not seriously distorted, and there is no stress concentration phenomenon.

Next, the tangential, radial, and axial stress and strain of the pipe are analyzed.

As shown in Fig. 9, during the setting-round, the outer layer of the positive bending area is stretched, and the inner layer is compressed. On the contrary, the outer layer of the reverse bending area is compressed, and the inner layer is stretched. The tangential strain of the neutral layer is very small and can be approximated to zero.

The tangential direction is also the main stress direction. The tangential stress of the inner and outer layers of the pipe end is extracted during the setting-round stage and after the setting-round, as shown in Fig. 10. It can be seen that in the setting-round stage, there are three positive bending areas and three reverse bending areas, and the tangential stress of the inner and outer layers is distributed in a "wavy" shape along the circumferential direction. Each positive and reverse bending area exists two peak stresses, the two

Fig. 9 The tangential strain distribution of the pipe end in the setting-round stage
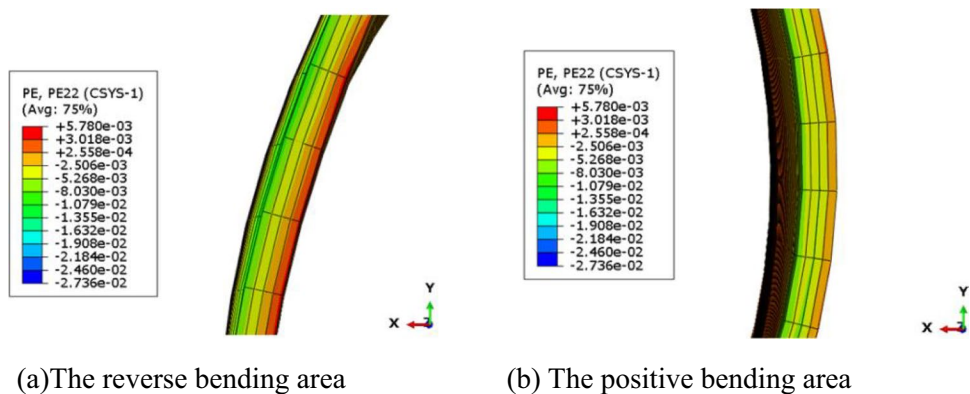

(a) The reverse bending area

(b) The positive bending area

Fig. 10 The tangential stress in the circumferential direction on the inner and outer surfaces at the pipe end
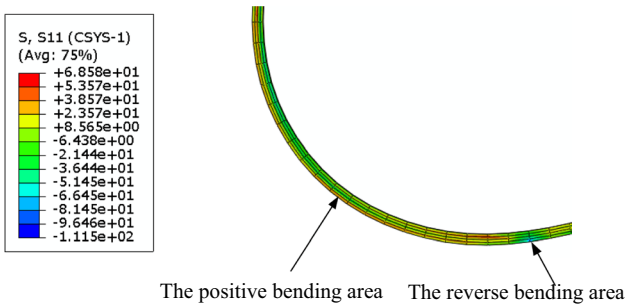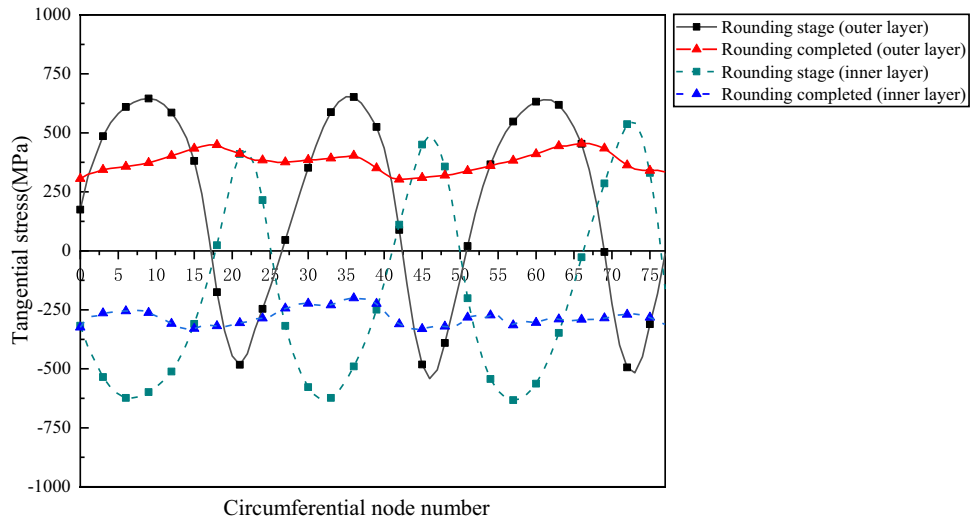

Fig. 11 The radial stress distribution of the pipe end in the setting-round stage
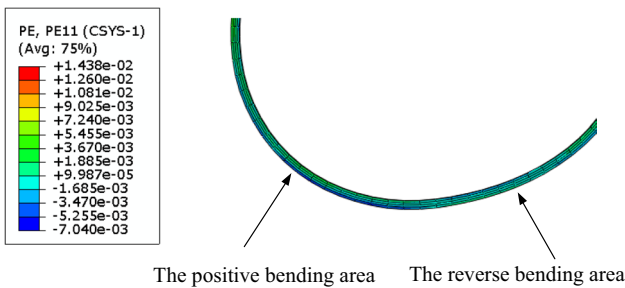

Fig. 12 The radial strain distribution of the pipe end in the setting-round stage

peak stresses are located at the midpoint of the positive and reverse bending area. After the setting-round is completed, the tangential stress of the inner and outer layers is greatly reduced, and the distribution is uniform.

Figures 11 and 12 show the distribution of radial stress and strain at the pipe end in the positive and reverse bending areas during the setting-round stage.

It can be seen from Fig. 11 that the radial stress is small, much lower than the yield stress 530 MPa. It can be seen from Fig. 12 that the radial strain value of the pipe end in the radial direction is small in the setting-round stage, so it can be considered that the radial geometry of the pipe end does not change during the setting-round process.

Figure 13 shows the distribution of the axial stress of the pipe end in the positive and reverse bending areas during the setting-round stage. It can be seen from Fig. 13 that the axial stress is very small compared to the yield stress. Therefore, it can be considered that the pipe end does not undergo plastic deformation in the axial direction during the setting-round process.

5.1.2 Effects of roller taper on setting-round results

During the modeling process, the roller taper was set to 0.2, 0.4, and 0.67. A straight pipe of X70 material with a nominal outer diameter of 100 mm, a thickness of 2 mm, and an initial ovality of 3.14% was selected for simulation, and the results are shown in Fig. 14.

It can be seen from Fig. 14 that under the same taper, the residual ovality decreases with the increase of the reduction. Under the same reduction, the change of the roller taper has little effect on the residual ovality. When the roller taper is 0.2, the residual ovality is small. Therefore, the roller taper is set to 0.2.

5.1.3 Effects of forward speed on setting-round results

On the basis of excluding the effect of the roller taper, it is necessary to further explore the effect of the forward speed on the setting-round results. A straight pipe of X70 material with a nominal outer diameter of 100 mm, a thickness of 2 mm, and an initial ovality of 3.14% was selected for

Fig. 13 The axial stress distribution of the pipe end in the setting-round stage
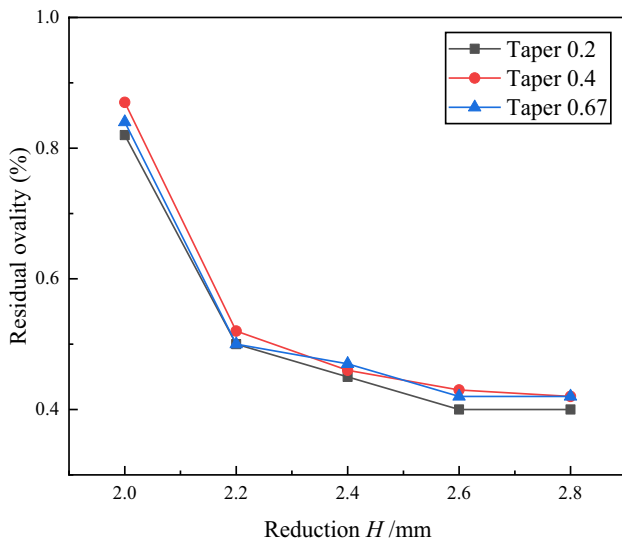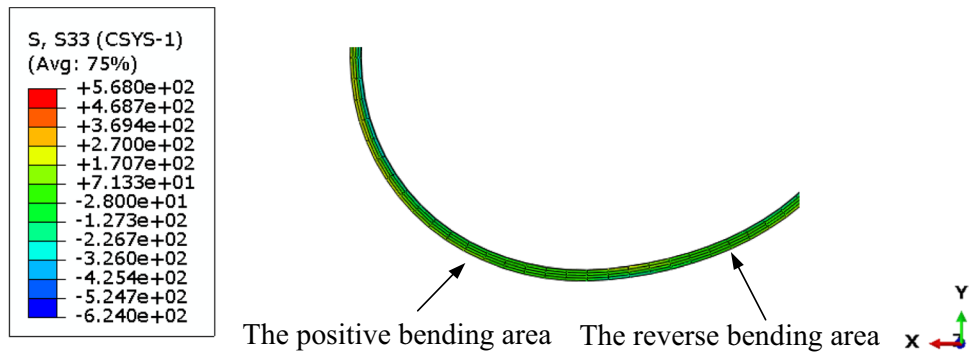

The positive bending area   The reverse bending area

Fig. 14 Relationship between the reduction and the residual ovality under different roller tapers

Fig. 15 Relationship between the reduction and the residual ovality under different forward speeds

simulation. In the simulations, the forward speeds of the three rollers were set as 2 mm/s, 3 mm/s, and 4 mm/s, respectively. Figure 15 shows the relationship between the reduction and the residual ovality when the forward speed is different.

It can be seen from Fig. 15 that at the same forward speed, with the increase of the reduction, the residual ovality shows a decreasing trend. Under the same reduction, the residual ovality does not change significantly when the forward speed is different. However, when the speed is too fast, the collision between the rollers and the pipe will cause stress concentration on the edge of the pipe end, resulting in the deformation of the pipe. Therefore, the forward speed is selected as 2 mm/s.

5.1.4 Effects of reduction on setting-round results

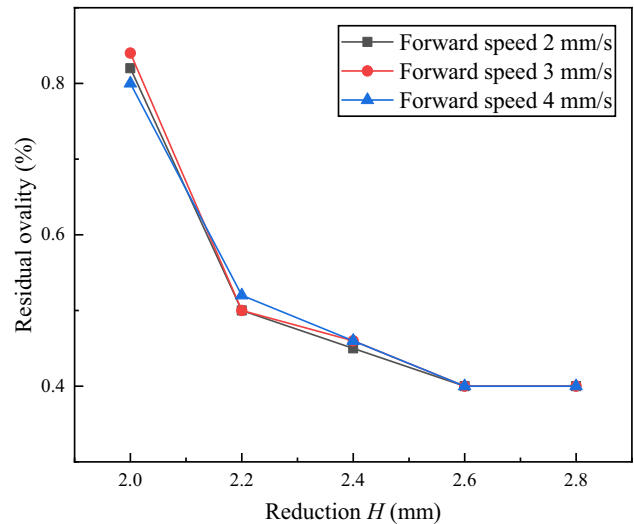The straight pipes of X70 and X80 materials with a nominal outer diameter of 100 mm, a thickness of 2 mm, and an initial ovality of 3.14% were selected for simulation. The data obtained from the simulations are shown in Fig. 16.

It can be seen from Fig. 16 that the residual ovality of X70 and X80 materials can reach a minimum of 0.4%, which is in line with API standards. The residual ovality decreases with the increase of the reduction, and when the reduction reaches a certain value, the residual ovality basically does not change. The optimum reduction of 100 mm X70 and X80 materials straight pipe are 2.6 mm and 2.8 mm, respectively. The residual ovality of the X70 and X80 pipes under the optimum reduction is 0.40% and 0.42%, respectively. The relationship between the reduction and the residual ovality of the straight pipes with nominal outer diameters of 120 mm and 140 mm was investigated, as shown in Fig. 17.

It can be seen from Fig. 17 that the optimal reduction of 120 mm straight pipe of X70 material is 3.2 mm, and the optimal reduction of 140 mm straight pipe is 3.6 mm. The optimal reduction of 120 mm straight pipe of X80 material
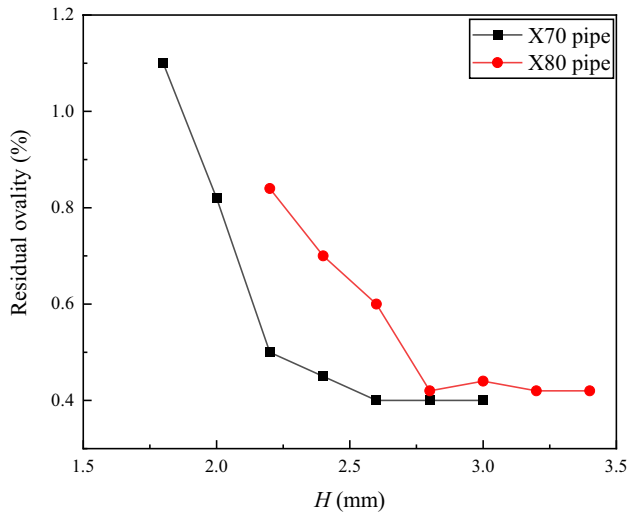
Fig. 16 Relationship between the reduction and the residual ovality for X70 and X80 materials
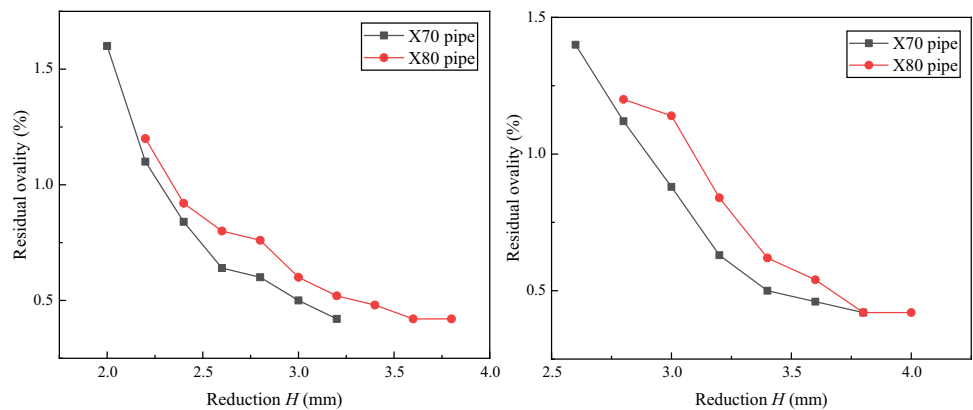
is 3.6 mm, and the optimal reduction of 140 mm straight pipe is 3.8 mm.

5.1.5 Effects of initial ovality on setting-round results

The straight pipes with nominal outer diameter of 100 mm, thickness of 2 mm, and X70 and X80 materials were selected as the research objects. The initial ovality in the simulation is 1.6%, 2.2%, 2.5%, and 3.14%, respectively. The simulation results are shown in Fig. 18.

It can be seen from Fig. 18 that for pipes with different initial ovality, the difference in the residual ovality is small. The results show that the pipe fittings with different initial ovality can achieve good rounding effect under the same process parameters.

5.1.6 Effects of relative thickness on optimum reduction

According to the simulation results in Sect. 5.1.4, the optimum reduction for different sizes of pipes can be obtained. The simulation data is sorted and analyzed, and the relationship between the relative thickness and the optimal reduction is shown in Fig. 19.

It can be seen from Fig. 19 that with the increase of the relative thickness, the optimal reduction shows a downward trend, and the relationship between the relative thickness and the optimal reduction is approximately linear.

5.2 T-shaped straight tee

As shown in Fig. 20, the main dimensions of the T-shaped straight tee are the outer diameter of the end D_e, the length of the main pipe F, the height of the branch pipe E, and the wall thickness t.

The distance between the main pipe and the branch pipe of the tee is relatively close, so when the pipe end of the main pipe (branch pipe) is rounded, it will have a certain effect on the branch pipe (main pipe) due to the involved deformation. Therefore, it is not only necessary to study the effect of process parameters on the pipe end, but also to comprehensively consider the effect of parameter changes on the ovality of the adjacent pipe end. The dimensions of the T-shaped straight tee and the three rollers are shown in Table 3.

Tees require that the ovality of the three pipe ends meet the API standard, and there are three cases of unqualified ovality:

(1) The ovality of the main and branch pipes is not up to standard.
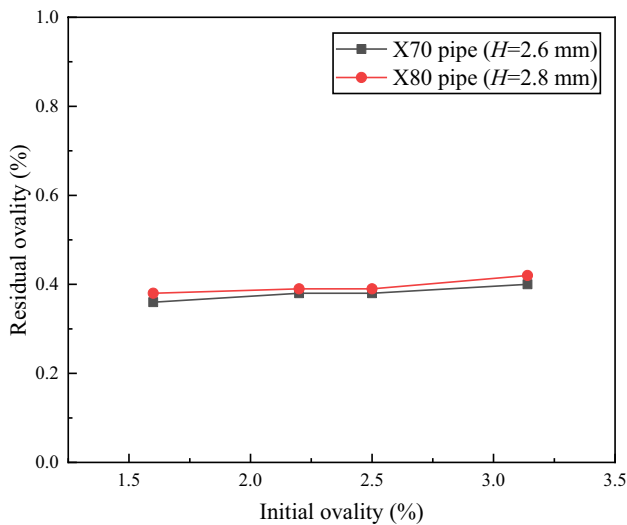(2) The ovality of the main pipe meets the standard, and the ovality of the branch pipe does not meet the standard.

Fig. 17 Relationship between the reduction and the residual ovality for 120 mm and 140 mm pipes

(a) 120 mm pipe

(b) 140 mm pipe

Fig. 18 Relationship between the initial ovality and the residual ovality under optimum reduction
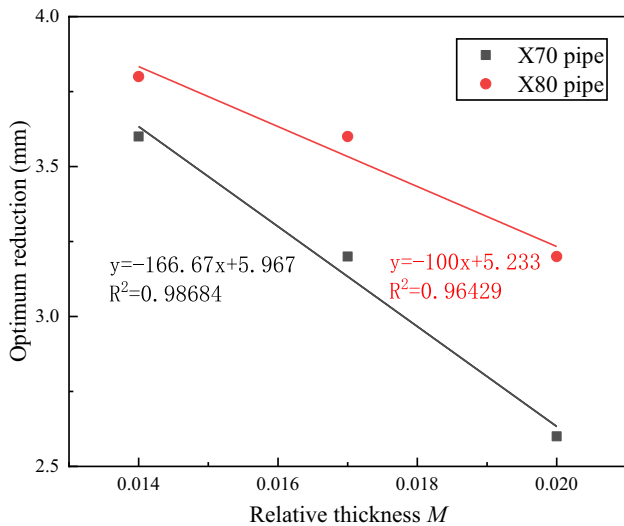
Fig. 19 Relationship between the relative thickness and the optimum reduction

Fig. 20 T-shaped straight tee dimension drawing

Table 3 Dimensions of T-shaped straight tee and rollers in pipe end setting-round process

D_e (mm)	t (mm)	F (mm)	E (mm)	C	L_r (mm)
100	2	149.8	74.9	0.4	65

where D_e is the outer diameter of the end, t is the wall thickness, F is the length of the main pipe, E is the height of the branch pipe, C is the taper of the roller, and L_r is the roller length

(3) The ovality of the branch pipe is up to the standard but the ovality of the main pipe is not up to the standard.

Among them, situation 1 is the most complicated. In view of this situation, the setting-round flow chart is drawn, as shown in Fig. 21.

First, the ovality of the branch pipe is measured to determine its compliance. If the ovality of the branch pipe does not meet the standard, the appropriate reduction is selected to round the branch pipe. Then, the ovality of the main pipe is measured to determine its compliance. If the ovality of the main pipe meets the standard, the
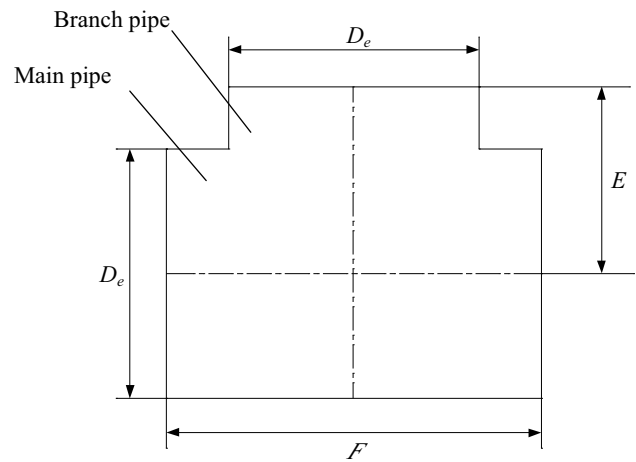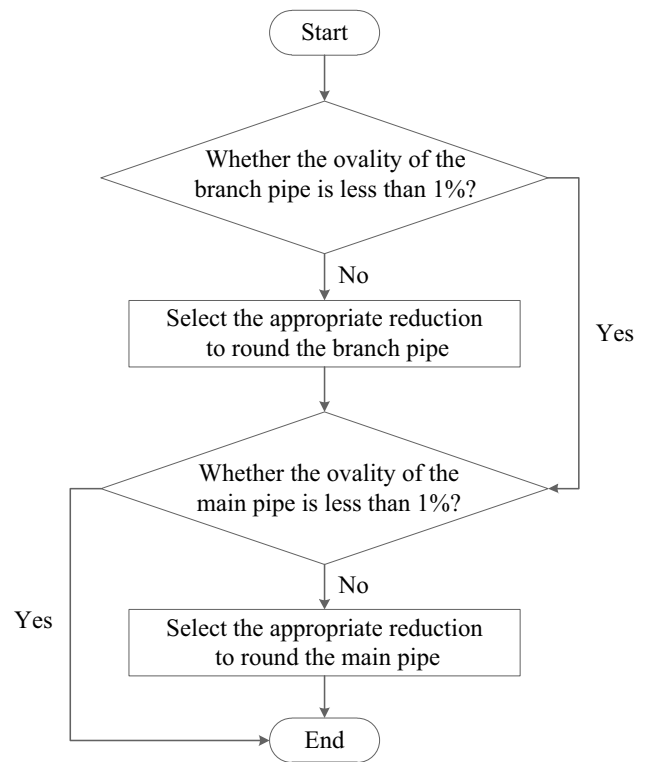

Fig. 21 T-shaped straight tee setting-round flow chart

setting-round is ended. If the ovality of the main pipe does not meet the standard, the appropriate reduction is selected for setting-round the main pipe. In this process, in order to avoid too much effect on the qualified branch pipe when setting-round the main pipe, an appropriate reduction should be selected.

Next, the tee made of X70 material is selected for simulation. The initial ovality of the main pipe and the branch pipe are both 3.2%, and the same reduction is set for the main pipe and the branch pipe. The branch pipe is rounded under different reductions, and the residual ovality data of the branch pipe and the main pipe after setting-round are shown in Fig. 22.

As shown in Fig. 22, when the reduction is within 1.8 to 2.4 mm, the ovality of the branch pipes after setting-round is less than 1%, which meets the API standard. At this time, the residual ovality of the main pipe changed, and the ovality after the change was between 2.8% and 3.2%. The residual ovality of the main pipe does not meet the standard, so the main pipe needs to be rounded. Figure 23 shows the residual ovality data of the main pipe and branch pipes after setting-round the main pipe.

As shown in Fig. 23, within the reduction of 1.8 to 2.4 mm, the residual ovality of the main and branch pipes is less than 1%, which meets the API standard. The residual ovality of the main and branch pipes first decreased and then increased. The setting-round results are best when the reduction is 2 mm. To sum up, within a suitable reduction range, the ovality of the main pipe and the branch pipe can be guaranteed. Therefore, it can be considered that this process has a good and stable effect on the setting-round of the tee.
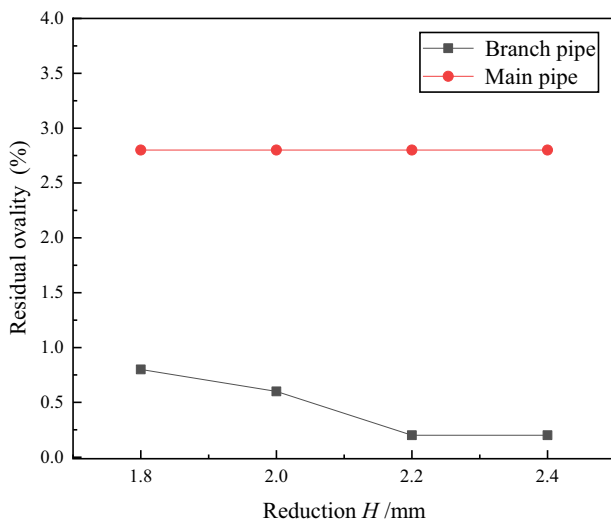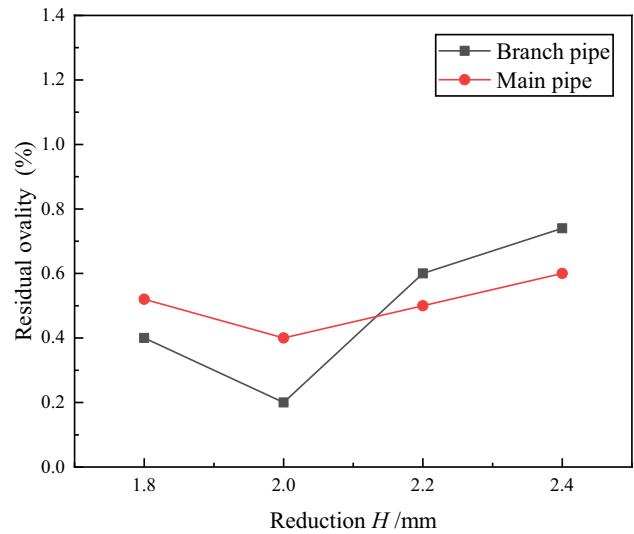

Fig. 23 Relationship between residual ovality of branch and main pipe and reduction

5.3 90° elbow with straight sections

As shown in Fig. 24, the main dimensions of a 90° elbow with straight section are the outer diameter of the end D_e, the height from the center to the end face A, the length of the straight section L_s, the radius of curvature K, and the wall thickness t. The dimensions of the 90° elbow with straight section and the three rollers are shown in Table 4.

The elbow is an arc-shaped pipe with a certain curvature, and the length of the straight section is small. Therefore, when rounding the pipe end, the arc portion of the elbow may be affected. From the simulation results, it is known
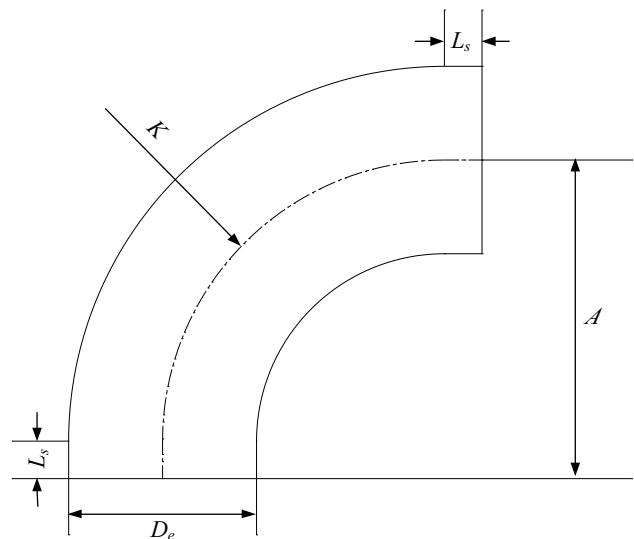

Fig. 22 Relationship between the residual ovality of the branch and main pipe and reduction

Fig. 24 90° elbow with straight section dimension drawing

Table 4 Dimensions of 90° elbow with straight section and rollers in pipe end setting-round process

D_e (mm)	t(mm)	A (mm)	K(mm)	L_s (mm)	C	L_r (mm)
100	2	160	150	10	0.38	75

where D_e is the outer diameter of the end, t is the wall thickness, A is the height from the center to the end face, K is the radius of curvature, L_s is the length of the straight section, C is the taper of the roller, and L_r is the roller length
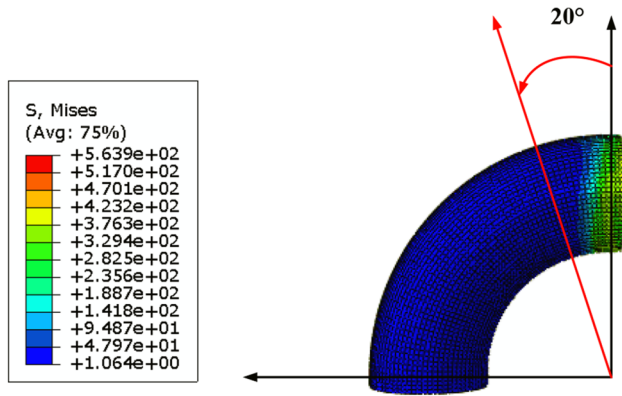

Fig. 25 The equivalent stress distribution of the elbow after setting-round

Fig. 26 Variation of ovality with angle under different reductions

Table 5 Setting-round data of elbow under different reductions

Material	Initial ovality β_0 (%)	Reduction H (mm)	Residual ovality β_1 (%)
X70	3.14	2	0.58
		2.2	0.5
		2.4	0.42
		2.6	0.42

From the data in Table 5, it can be seen that the residual ovality is smaller when the reduction is 2.4 mm and 2.6 mm. In order to observe the change of the overall ovality of the pipe after setting-round, the data of the ovality change for the arc part were organized. The residual ovality of different angles in the arc part under different reductions is shown in Fig. 26.

It can be seen that under different reductions, the ovality of the arc part of the elbow changes slightly. Except for the reduction of 2.6 mm, the ovality changes under the other reductions are all less than 1%. Therefore, it can be considered that this process can guarantee the setting-round effect of the elbow.

6 Experiments

6.1 Experimental setup

The experimental setup is shown in Fig. 27. The experiments were carried out on a CNC machine. The core part of the device is the setting-round die and the fixed Morse chuck. The setting-round die is clamped on the main shaft by the three-jaw chuck, which can realize the rotation movement. The fixed Morse chuck is assembled

that the residual ovality after the setting-round of the elbow is 0.42% when the reduction is 2.4 mm, which is in line with the API standard. Its equivalent stress distribution is shown in Fig. 25.

It can be seen from Fig. 25 that after setting-round, the pipe end and pipe body are not seriously distorted, and there is no stress concentration phenomenon. The deformation of the bent portion of the elbow is mainly concentrated in the range of 20° counterclockwise rotation from the starting position of the arc part. Therefore, in the process of setting-round the end of the elbow, it is not only necessary to study the influence of the reduction on the end setting-round result, but also to comprehensively study the influence of the reduction on the curved part. Table 5 shows the ovality data of the pipe end after setting-round of X70 material pipe with different reductions.
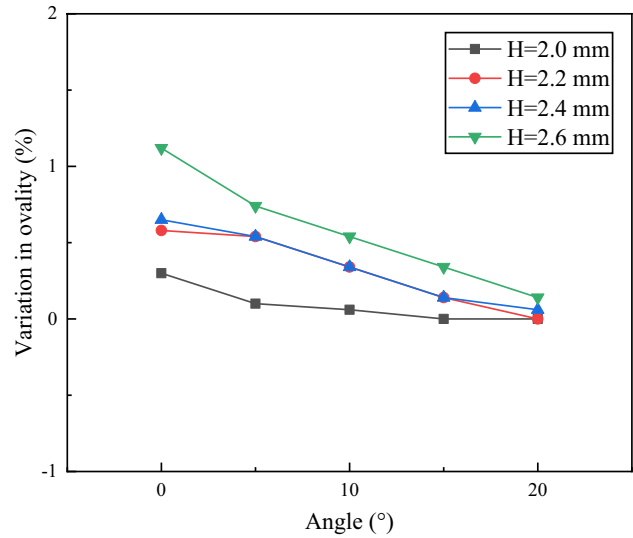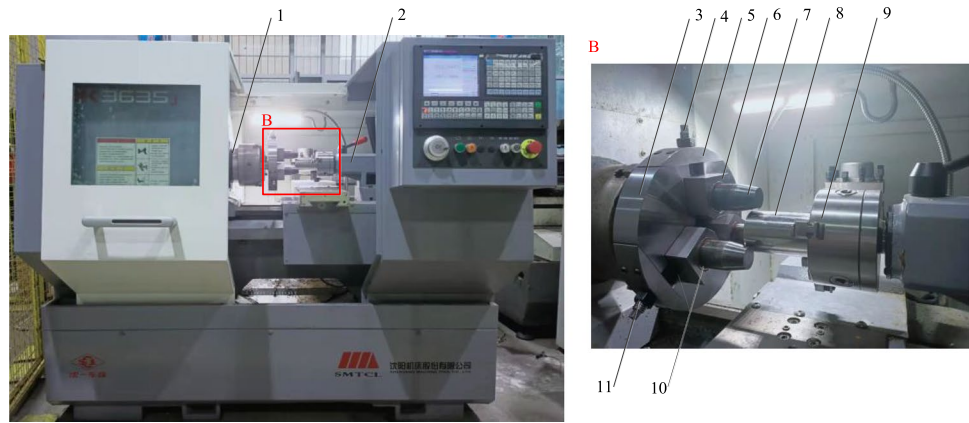
Fig. 27 Setting-round experimental setup. 1. Spindle; 2. Tailstock; 3. Turntable; 4. Lead screw; 5. Screw seat; 6. Slider; 7. Roller; 8. Pipe; 9. Fixed Morse chuck; 10. Bearing; 11. Set nut

on the tailstock, which can clamp and drive the pipe for translation.

The lead screw passes through the screw seat and is assembled with the slider through a bearing, which can control the movement of the slider. The rollers are assembled on the slider through bearings, and can rotate under the action of friction. The distance between the rollers can be adjusted by the movement of the slider. The diameter of the rollers is 40 mm, and the taper is 0.33. To prevent the slider from shaking during the setting-round process, a set nut is installed on the upper end of each lead screw. In the experiments, the straight pipes of 304 stainless steel were selected, and the length, thickness, and nominal outer diameter were 100 mm, 1 mm, and 60 mm, respectively. Pipes with different initial ovality were prepared by pressing method. Ovality of the pipe ends before and after setting-round was measured by using the 3000iTM series portable three-coordinate measuring instrument produced by CimCore Corporation of the United States.

6.2 Results and discussion

The experimental results obtained under different parameters are shown in Table 6. It can be seen from EXP1-EXP4

that when the reduction is between 0.8 and 1.4 mm, residual ovality of the pipe ends is less than 1%, which meets the API 5L standard. Residual ovality shows a decreasing trend with the increase of the reduction. When the reduction is 1.2 mm, residual ovality reaches a minimum value of 0.31%. It can be seen from EXP3, EXP5, and EXP6 that under the same process parameters, pipes with different initial ovality have good setting-round effects, residual ovality is between 0.31 and 0.61%, and the deviation is not large. The pipes after setting-round are shown in Fig. 28. It can be seen that ovality of the pipe ends is good, and there is no defect such as wrinkling and cracking.

7 Conclusions

In view of the limitations of the existing setting-round processes, a new setting-round process of pipe ends by three-roller was proposed. Considering the Bauschinger effect, the yield plateau phenomenon, and the variation of elastic modulus, numerical simulation and experimental methods were applied to verify the feasibility of the process and to
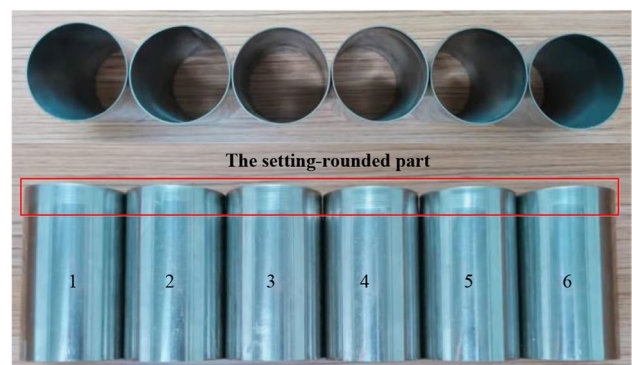
Table 6 Residual ovality results from experiments

Material	Numbering	Initial ovality β_0 (%)	Reduction H (mm)	Residual ovality β_1 (%)
304	EXP1	2.46	0.8	0.61
	EXP2	3.82	1	0.4
	EXP3	2.18	1.2	0.31
	EXP4	2.78	1.4	0.34
	EXP5	1.12	1.2	0.35
	EXP6	4..4	1.2	0.61

Fig. 28 A picture of the pipes after setting-round

explore effects of process parameters. The main conclusions are as follows:

(1) The finite element results and experimental results both verified the feasibility of the new process. Residual ovality of pipes with unqualified ovality after setting-round is all within 1%, which is in line with API standards. The new process can realize continuous setting-round of pipe ends for different types of pipe fittings, and the setting-round efficiency is high.

(2) Residual ovality first decreased and then stabilized with the increase of reduction. Initial ovality has little effect on the setting-round results, and the pipes with different initial ovality were well rounded under the same reduction.

(3) Different materials have different optimal reductions, and the optimal reduction increases with the increase of yield strength. The optimal reduction is linearly related to the relative thickness, so that the optimal reduction at different relative thicknesses can be predicted.

(4) When setting-round the tee pipes and elbows with straight sections, the setting-round of pipe ends has little effect on the other parts of pipes, and a good setting-round effect can be achieved.

(5) The modified Chaboche hardening model with three back stresses combined with the chord modulus model has good description accuracy for the hysteresis curve of materials with the yield plateau. The realization of this material model in finite element software can provide reference for simulations of other processes involving reciprocating bending.

Declarations

Competing interests The authors declare no competing interests.

References

1. Ansi/Api Specification 5L, Forty-foruth Edition (2009) Washington DC: Specification for Line Pipe.
2. Karrech A, Seibi A (2010) Analytical model for the expansion of tubes under tension. J Mater Process Tech 210:356–362. https://doi.org/10.1016/j.ijplas.2016.07.002
3. Zhao J, Yin J, Ma R, Ma LX (2011) Springback equation of small curvature plane bending. Sci China Technol Sci 54:2386–2396. https://doi.org/10.1007/s11431-011-4447-4
4. Yin J, Zhao J, Qu XY, Zhai RX (2011) Springback analysis of expanding diameter rounding for large pipe fittings. Chin J Mech Eng 47:32–42. https://doi.org/10.3901/JME.2011.12.032
5. Ji ZC, Zou TX, Ren Q, Li DY, Xin JY, Li XW, Guo Y (2014) Finite element simulation research on UOE welded pipe expanding process. Petroleum Machinery 42:111–115. https://doi.org/10.3969/j.issn.1001-4578.2014.05.025
6. Yin J, Zhao J, Sun HL, Zhan PP (2011) Precise compression setting-round by die for large pipes. Opt Precis Eng 19:2072–2078. https://doi.org/10.3788/ope.20111909.2072
7. Zhao J, Zhan PP, Ma R, Zhai RX (2012) Control strategy of over-bending setting round for pipe-end of large pipes by mould press type method. Trans Nonferrous Metals Soc China. https://doi.org/10.1016/S1003-6326(12)61727-0
8. Zhao J, Zhan PP, Cao HQ (2010) Prediction of optimal process parameters for inner expansion, bending and rounding of pipeline steel pipes. National Stamping Academic Annual Conference. Chin Mech Eng Soc
9. Yu GC, Zhao J, Ma R, Zhai RX (2016) Unified curvature theorem for reciprocating bending and its experimental verification. Chin J Mech Eng 52:57–63
10. Xing JJ (2014) Research on three-roll rounding technology. Yanshan University
11. Yu GC, Zhao J, Xing JJ, Zhao FP, Li LL (2017) Research on symmetrical three-roll rounding process. Chin J Mech Eng 53:136–143. https://doi.org/10.3901/JME.2017.14.136
12. Huang XY, Zhao J, Yu GC, Meng QD, Mu ZK, Zhai RX (2021) Three-roller continuous setting round process for longitudinally submerged arc welding pipes. Trans Nonferrous Metals Soc China 31:1411–1426. https://doi.org/10.1016/S1003-6326(21)65586-3
13. Huang XY, Yu GC, Zhai RX, Ma R, Zhou C, Gao CL, Zhao J (2021) Roll shape design and process simulation of three-roll continuous composite orthopedic process for large-scale longitudinally welded pipes. Chin J Mech Eng 57:148–159. https://doi.org/10.3901/JME.2021.10.148
14. Prager W (1956) A new method of analyzing stresses and strains in work-hardening plastic solids. Int J Appl Mech 23. https://doi.org/10.1115/1.4011389
15. Ziegler H (1959) A modification of prager's hardening rule. Q.appl.math 17:55–65
16. Mróz Z (1967) On the description of anisotropic workhardening. J Mech Phys Solids 15:163–175. https://doi.org/10.1016/0022-5096(67)90030-0
17. Armstrong PJ, Frederick CO (1966) A mathematical representation of the multiaxial Bauschinger effect. G.E.G.B repor; RD/B/N 731
18. Chaboche JL (1986) Time-independent constitutive theories for cyclic plasticity. Int J Plast 2:149–188. https://doi.org/10.1016/0749-6419(86)90010-0
19. Zou TX (2016) Forming modeling and process robust design of high-strength UOE steel pipes. Shanghai Jiaotong University, Shanghai
20. Zobec P, Klemenc J (2021) Application of a nonlinear kinematic-isotropic material model for the prediction of residual stress relaxation under a cyclic load. Int J Fatigue. https://doi.org/10.1016/j.ijfatigue.2021.106290
21. Hai LT, Li GQ, Wang YB, Wang YZ (2021) A fast calibration approach of modified Chaboche hardening rule for low yield point steel, mild steel and high strength steels. J Build Eng 38:102168. https://doi.org/10.1016/j.jobe.2021.102168
22. Yoshida F, Uemori T, Fujiwara K (2002) Elastic–plastic behavior of steel sheets under in-plane cyclic tension–compression at large strain. Int J Plast 18:633–659. https://doi.org/10.1016/S0749-6419(01)00049-3

23. Yoshida F, Uemori T (2003) A model of large-strain cyclic plasticity and its application to springback simulation. Key Eng Mater 233–236:47–58. https://doi.org/10.4028/www.scientific.net/KEM.233-236.47

24. Eggertsen PA, Mattiasson K (2009) On the modelling of the bending-unbending behavior for accurate springback predictions. Int J Mech Sci 51:547–563. https://doi.org/10.1016/j.ijmecsci.2009.05.007

25. Yilamu K, Hino R, Hamasaki H, Yoshida F (2010) Air bending and springback of stainless steel clad aluminum sheet. J Mater Process Tech 210:272–278. https://doi.org/10.1016/j.jmatprotec.2009.09.010